IAC–23–D1,2,11,x77783

Concept and design of an autonomous micro rover for long term lunar exploration

Niklas A. Mulsow[a]**, Benjamin Hülsen**[a]**, Joel Gützlaff**[b]**, Leon Spies**[b]**, Andreas Bresser**[a]**, Adam Dabrowski** [a]**, Markus Czupalla**[b]**, Frank Kirchner**[ac]

[a] *DFKI GmbH, Robotics Innovation Center, Bremen, Germany*
[b] *FH Aachen University of Applied Sciences, Germany*
[c] *FB3 - Robotics Research Group, University of Bremen, Germany*

Abstract

Research on robotic lunar exploration has seen a broad revival, especially since the Google Lunar X-Prize increasingly brought private endeavors into play. This development is supported by national agencies with the aim of enabling long-term lunar infrastructure for in-situ operations and the establishment of a moon village. One challenge for effective exploration missions is developing a compact and lightweight robotic rover to reduce launch costs and open the possibility for secondary payload options. Existing micro rovers for exploration missions are clearly limited by their design for one day of sunlight and their low level of autonomy. For expanding the potential mission applications and range of use, an extension of lifetime could be reached by surviving the lunar night and providing a higher level of autonomy. To address this objective, the paper presents a system design concept for a lightweight micro rover with long-term mission duration capabilities, derived from a multi-day lunar mission scenario at equatorial regions. Technical solution approaches are described, analyzed, and evaluated, with emphasis put on the harmonization of hardware selection due to a strictly limited budget in dimensions and power.

1. Introduction

Lunar operations are critical to achieving key future science and exploration objectives. However, the lunar day-night cycle, which includes fourteen Earth days of sunlight followed by fourteen Earth days of darkness, poses one of the greatest technological challenges to achieving a sustainable presence on the Moon. While sunlight provides the energy to run the system during the day, energy is needed to maintain heating during the night to prevent the system from freezing. Temperatures on the lunar surface can reach values between approx. +120 °C during the day time and -170 °C at night [1].

Thus, one of ESA's key elements for lunar science [2] is the development of technologies for surviving lunar nights and for night time operations. It will also require a robust control system that supports the operator, works without a direct radio link and has semi-automation guidance navigation and control (GNC) capabilities. This will also help to enable future lunar missions to explore permanently shadowed areas and enhance operational and exploration capabilities in the Solar System.

Because mass is one of the most important factors in mission cost, micro-rover applications demonstrate comparably low monetary expenditure. Enabling night survival and operation in shaded areas would increase their value considerably, especially in long duration missions and swarm exploration scenarios. They also provide a suitable payload for landers being developed by the private space industry, increasing the likelihood of launch opportunities.

1.1 State of the Art

Micro rovers are systems with a comparably small total mass. The mass limit to classify a rover vehicle as a 'micro rover' is not clearly defined [3]. While some sources set the limit at 10 kg [4], other literature states a more qualitative upper weight limit of 'a few kilograms' [5]. To make a clear distinction we draw the line at 30 kg.

Figure 1 shows competitors for being the first micro rover to be landed on the lunar surface in the mid 2020s. The first missions for testing the iSpace lander in April 2023 including UAE's rashid rover, as well as the Chandrayaan-2 mission in 2019, ended in a crash on the lunar surface. As we now know by
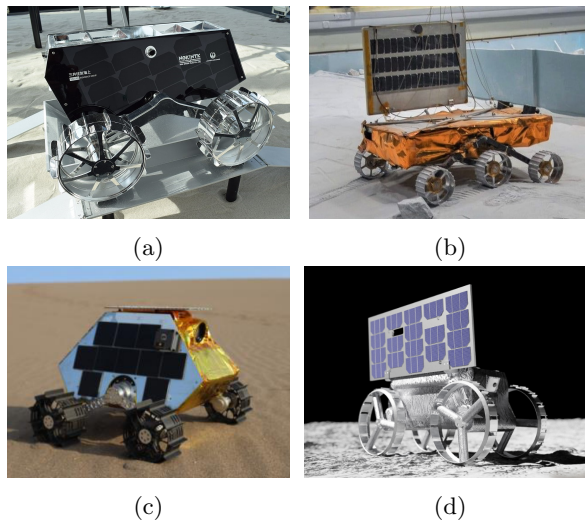
(a)

(b)

(c)

(d)

Fig. 1: Systems with envisaged landing on the moon in the mid 2020s: *a:* HAKUTO (iSpace [7]); *b:* Chandrayaan-3 rover (ISRO); *c:* MAPP (Lunar Outpost); *d:* Cube-Rover (Astrobotic [8])

ISRO, the Chandrayaan-3 rover has been successfully deployed from the Vikram lander and is operating on the Moon.

However, none of these systems would be able to survive the lunar night, but efforts are underway to achieve this. Lunar Outpost is working on a version of the MAPP rover [6] with a mass of about 15 kg, using batteries and LiDAR technology to drive and navigate for long periods in permanently shadowed regions (PSR). For heat generation, Astrobotic presented the NITE heat generation system based on chemical reactions, which could be used on a lander and a rover.

1.2 Motivation and Objectives

Rovers that can only operate in daylight are limited to a maximum mission duration of about fourteen Earth days. A rover capable of surviving the night phase would therefore multiply mission duration, travel distance and operating range. This would allow more mission objectives to be achieved in a single step, reduce the cost per distance travelled and increase the area explored. For that, concepts of thermal control systems are discussed and evaluated in the SAMLER-KI* project at the FH Aachen and DFKI Bremen.

An approach to lunar rover system design is de-

***

*https://robotik.dfki-bremen.de/de/forschung/projekte/samler-ki
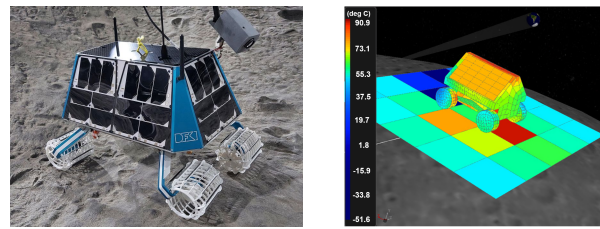

Fig. 2: Rover MoVe in DFKI's space exploration hall [10]

Fig. 3: Simulation of the MoVe rover on lunar surface with Thermica v4 [11]

scribed that includes a thermal control system (TCS) with innovative solutions using both passive and active means of thermal control. In addition, thermoelectric operating strategies are presented as a promising approach to support the control efforts given the tremendous variations in temperature and illumination during a lunar cycle. A low power hardware and software architecture for the GNC is also presented, including a selection of sensors and the bus topology for the on-Board data handling (OBDH).

1.3 Previous Work

DFKI can draw on preliminary work from the SEARCH project. There, different storage technologies [9] for a small lunar rover were investigated and the system design for a lunar daytime mission was developed (Figure 2). The rover, called MoVe, has a mass of 5.9 kg and is able to operate in sunlight without the need for chemical batteries to reduce its susceptibility to thermal fluctuations. The shape of the rover was analysed in a thermal simulation (Figure 3) and adapted to a mid-latitude range.

2. Mission

The rover system design presented in the following Section 3 is tailored for a lunar mission of at least 2 lunar days, including one night survival on the Aristarchus Plateau in the neat at the entrance to Cobra Head. It is designed to navigate semi-autonomously during communication timeouts and when crossing shaded areas. Its payload mass is limited by design to 500 g, so the primary objective is to acquire images, collect surface information and generate detailed surface maps to find points of interest for future missions. Table 1 summarises the key requirements for the system. A detailed description of the mission is given in [12].

Table 1: Systems key requirements

Requirement	Description	Value
Mission	Duration	min. 2 lunar days
	Travel distance	>250 m per lunar day
	Landing Site	Lat. 0°- 30°
Physical	System mass	<20 kg
	Rover speed	max 0,1 ms^{-1}
	Maximum boulder height to climb	15 cm
Functional	Take pictures and videos	FHD resolution max.
	Payload	0,5 kg (Imager, Spectrometer)
	Navigation	semi autonomous
Power	Solar powered	⌀ 15 W
COM	Lander	256 kBit/s Telemetry, 1 MBit/s High Speed Link

Fig. 4: Preliminary rover concepts for the SAMLER-KI rover

3. System concept

Two aspects have a significant impact on the design of the rover to achieve night survival and autonomous GNC: First, the influence of the TCS and electrical power system (EPS). Second, the design of the GNC and OBDH subsystems, as these are critical for system autonomy. A thermal demonstrator model shall be designed to test the TCS. The GNC stack will be tested under laboratory lighting conditions with a second functional demonstrator model. For performance reasons, the GNC cameras will be equivalent to space hardware, and the computers used in the OBDH subsystem and the EPS will be based on CubeSat components. Functionally equivalent components and technologies will be selected for the locomotion system (LOC), Communication System (COM) and Payload (PL) to facilitate the TRL increase of single subsystems and concepts.

To bring the requirements and designs together, the system and mission parameters were collected in a concurrent design study. The resulting relationships can be broken down into generic design premises:

Keep the design simple Avoiding additional actuators, folding mechanisms and active elements helps to reduce mass and failure points. For the choice of sensors, LiDAR technology is omitted to keep the computational effort low and to ensure verifiability. Reducing component's size will help keeping the surfaces to be insulated small, which in turn reduces power loss at night and thus reduces mass.

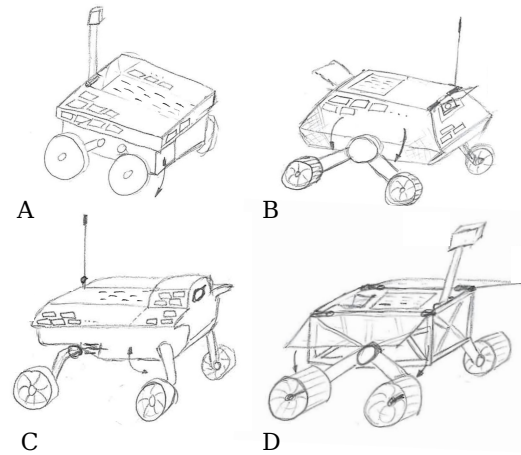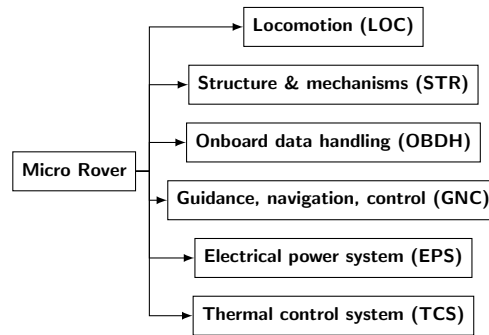**Reduce power consumption** Each subsystem is designed to consume as little power as possible. This

Fig. 5: System breakdown

results in fewer solar cells, less radiator area, a smaller system footprint, more flexibility in mission operations and an increase in operational time.

Reduce power losses throughout the night by design Overnight power losses require a large energy storage to compensate them. Continuous power losses of few watts already have a significant impact on system mass, as shown in Section 4.

3.1 System configuration

Different configurations for the shape of the body have been compared, as this has a large impact on the placement of solar cells and radiators, as well as the accommodation of the locomotion system. Active folding mechanisms such as a mast or a shutter will be omitted later, in order to keep the system as simple as possible. The rover is divided into the subsystems shown in Figure 5. The following sections describe these subsystems in detail and the design choices made for each.
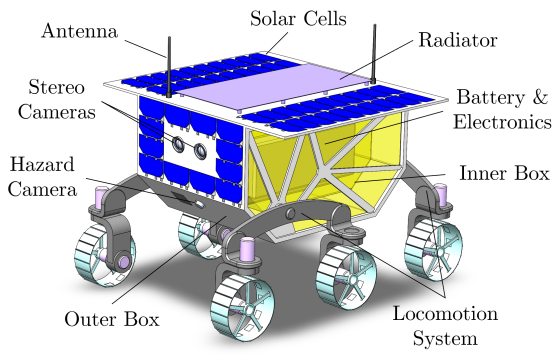
Fig. 6: Illustration of the design approach of the SAMLER-KI rover

Fig. 7: Overview of the global TCS design

Influences for the solar cell arrangement (Section 5) and the locomotion system accommodation (Section 6) let us come to a modified design approach shown in Figure 6. All electrical components are intendet to fit into one compartment to reduce the need for heating. For insulation, the rover body consists of an outer and an inner structural shell, which are conductively and radiatively decoupled as described in Section 4. Cut-outs in the insulation are kept small and active heating is avoided wherever possible. With a flat top surface, the design provides sufficient space for a radiator, the main solar panels and antennas. In addition, the outer box is fitted with solar panels at the front and back to collect sunlight in the morning and evening. A lower chamfer of the body at the front an rear site allows two hazard detection cameras to view the wheels. The payload can be mounted next to the hazard detection camera in the front, providing the possibility of facing towards the ground if necessary.

Attached to the side, the locomotion system can be folded under the top solar panel for transport. The side structure allows suitable mounting points for release actuators or deployment mechanisms.

A six-wheeled design was chosen as this proved to be the most suitable, efficient and smallest design (see Section 6). To facilitate the navigation cameras' insulation, they are integrated directly into the rover's body.

4. Thermal Control System

From a thermal perspective, the lunar surface is a challenging environment. The lunar daytime, lasting approx. fourteen Earth days, shows ground temperatures of approx. 120 °C [1] and a direct solar flux of 1360 W/m^2. This is in sharp contrast to the lunar
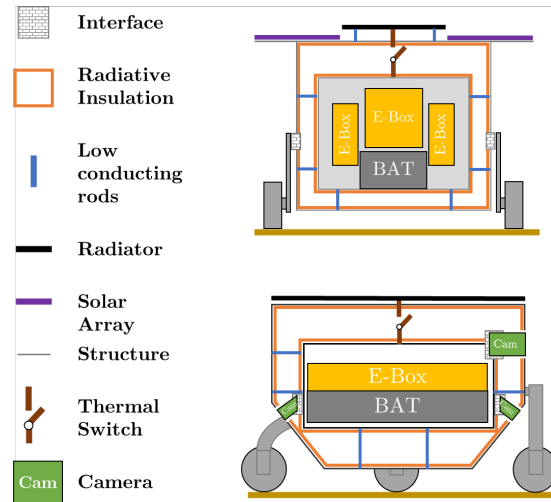
nighttime, as well about fourteen Earth days long, which is characterised by temperatures of down to -170 °C [1] with rapid cooling and heating during dusk and dawn respectively.

To cope with these circumstances, a TCS is to be developed with the objective of keeping the electronics of the rover in their operational ranges of approx. -40 °C up to +80 °C. Up to now, conceptual approaches have been developed and traded. Figure 7 shows a promising conceptual TCS approach developed for the SAMLER-KI rover. Extensive analyses remains to be done to demonstrate the feasibility and actual performance. In general, the design is influenced by the following parameters:

4.1 Heat Losses

Due to the cold environment above as well as around and below the rover in combination with the long nighttime, even small heat leaks result in large energy losses, which must be compensated for by active heating. A significant source of heat loss will be the entire rover surface. Thus, the objective is to radiatively and conductively decouple the rover's thermally sensitive components from its outer surface.

Cut-outs for e.g. cameras and sensors are thermal bridges through the insulation of the rover surface. Even more critical is the attachment of the locomotion system to the rover chassis, since it opens a conductive heat path to the large outer surface of the locomotion system as well as to the lunar surface directly. Another significant heat leak is present in the form of the radiator. As it is thermally well connected to the heat dissipating components to reject heat dur-
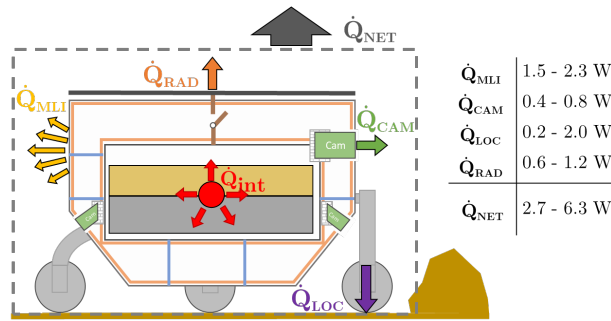
Fig. 8: Expected heat losses during night

ing the lunar day, it must be covered during the night or the heat path has to be reduced considerably.

An overview of the estimated heat losses during the nighttime for the conceptual approach mentioned above is given in Figure 8.

4.2 Energy storage

To compensate for heat losses during the night, electrical heaters shall be used at critical components. The amount of energy lost by heat leaks has to be stored in an electrical energy storage. State of the art batteries, as described later in Section 5, have effective energy capacities of around 190 W/kg. Assuming a constant heat loss of 4 W during the night-time would already yield a required battery capacity of 1610 Wh including a margin of 20 %, resulting in a mass of approx. 9 kg.

4.3 Insulation

The concept for radiatively insulating the rover is based on Multi-Layer Insulation (MLI). In general, the insulating capabilities improve with the number of layers, though the improvement continuously reduces and becomes insufficient with regard to mass increase after about 25 layers [13]. This can be further reduced by utilizing two sheets of MLI with spacing in between. Based on this rationale, a dual-box design for the rover shall keep apart two MLI sheets of 25 layers each. To separate the insulated inner box from the outer box, tube connectors with low conducting material properties, such as GFRP, shall be implemented (See Figure 7). The feasibility of this concept is yet to be shown by thermal as well as structural analyses.

Using literature values from [14] for high performance MLI, the heat loss for this dual-box approach with a surface completely covered in MLI is preliminarily estimated to be $1.5 - 2.3W$, compared to approx. $3.5 - 4.6W$ for a single box design. However,
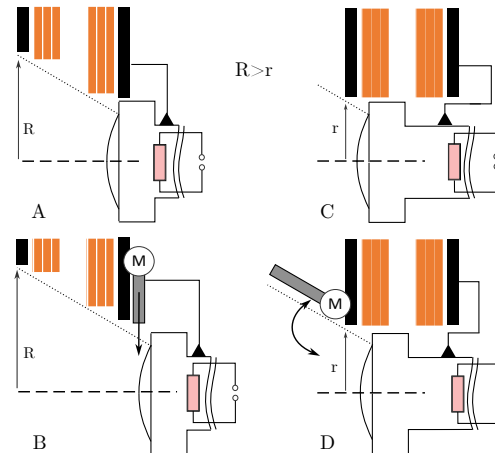

Fig. 9: Approaches for realizing the cutouts for cameras through the MLI-insulation: *A:* Placing the camera behind the MLI; *B:* Using an inside mounted shutter for extra insulation; *C:* (Favorite) Placing the camera lens in the outer plane of the MLI; *D:* Using an outside mounted shutter for extra insulation; Resistor (red) is for heating the sensors)

this does not comprise any cut-outs or conductive heat leaks.

Camera Cutouts The cutouts for the navigation and hazard detection cameras are a particular design challenge as they cause radiant heat losses at night. Figure 9 shows four design approaches. The first idea (*A*) of placing the cameras behind the insulation attached to the inner structure, proved unfeasible due to the increased cutout radius in the outer MLI insulation, as can be seen in Figure 9.

A second approach is to actively close the cameras with a cover (design *B* & *D*). However, there are challenges in finding suitable actuators and mounting them to prevent heat loss by conduction. It also carries a high risk of failure and would add mass to the system.

Considering the design premise from Section 3, the cutout design was chosen according to design *C*. By placing the cameras inside the insulation, the combined cutout area for all cameras is estimated to be 50 cm² in total. This would result in a maximum heat loss between 0.4 - 0.8 W during the night.

4.4 Heat Rejection

To reject waste heat dissipated by electrical components, a radiator on the topside is to be utilized. Its size is estimated to be up to 0.1 m^2 for the ex-

pected maximum heat disposal of 30 W. To reduce the radiator mass compared to a classical aluminium radiator, a graphite radiator shall be implemented. This way, a lower specific mass can be realized while the higher in-plane conductivity guarantees a uniform temperature distribution over the radiator, increasing its efficiency [15] [16].

4.5 Heat Distribution

Inside the rover, heat dissipated by components is transported to the radiator on defined paths. As mentioned in Subsection 4.1, this heat path has to be significantly reduced during the night. Such a variable heat transport capability may be achieved by implementing a thermal switch on the heat path between the components and the radiator. Thermal switches are not yet available as commercial of-the-shelf (COTS) components but custom-made only, and have already been used in different configurations for several space missions like the Mars exploration rovers [17]. Currently, conductive ratios of up to 1:110 can be realised [18].

5. Electrical Power System (EPS)

Similar to the TCS, the EPS will have a significant influence on the rover system design. The EPS board chosen for the rover is the CubeSat EPS Nano P60 from GomSpace, equipped with suitable inputs and outputs and having a comparatively low power consumption of approx. 1.14 W. For the operation of additional subsystems like the locomotion subsystem, it is necessary to design a custom 25-channel eFuse board.

5.1 Power budget

The Table 2 shows the planned power consumption for each subsystem. The peak values are not intended to be used in total. Due to the high battery capacity required for night survival, the power consumption may substantially exceed the power provided by the solar panels for a certain duration.

5.2 Power Generation

In order to provide the necessary power for the system during the mission day, a reference panel with a theoretical maximum power of 30 W was first defined using Azur 3G30A cells to compare different panel arrangements for different rover configurations as shown in Figure 4. For this purpose, the reference panel was simplified and divided into 3 segments as shown in Figure 10. The power over the lunar day

Table 2: Estimated power budget of the SAMLER-KI rover. All values in W, OPL: operational

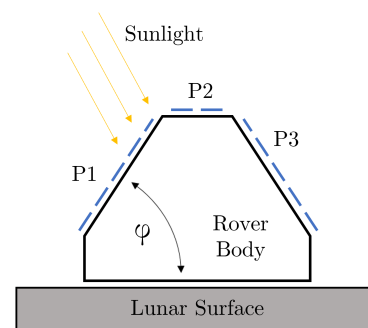| Components	Min	OPL	Max
Locomotion	5	10	25
OBDH	0,15	1,6	3,9
GNC	1,0	5,2	8,7
EPS	0,6	1,3	4,9
COM	0,7	3,1	15,6
TCS	0,1	1,0	5,0
Payload	0,0	2,0	5,0
Total	7,55	24,2	68,1

Fig. 10: Schematic for 2d solar panel placement on the rover

was then estimated for the different panel divisions and side panel angles φ (Figure 11).

Option 4 (purple curve) turned out to be the best compromise design for having nearly the same performance as a topside panel configuration while facilitating power input in the morning and evening. Additional to the main topside panel (P2), two side panels (P1 & P3) are considered. In the current design they are fitted to the rovers front and backside (Figure 6). They provide additional power in the morning and evening when the rover is aligned with the sun. This configuration also allows more space to be used on the surface of the rover than other configurations, as shown in Figure 4.

The configuration with two 30° panels also provides suitable performance characterisation, but needs more structural effort to implement. The pyramid design with two 60° panels as seen in the MAPP or Hakuto rover designs, shows a flattened power generation curve during the day at equatorial regions and was ruled out due to its low total energy gain (Figure 11). For the final demonstrator-implementation it is planned to use terrestrial cells with an efficiency of 25% but similar string voltage.
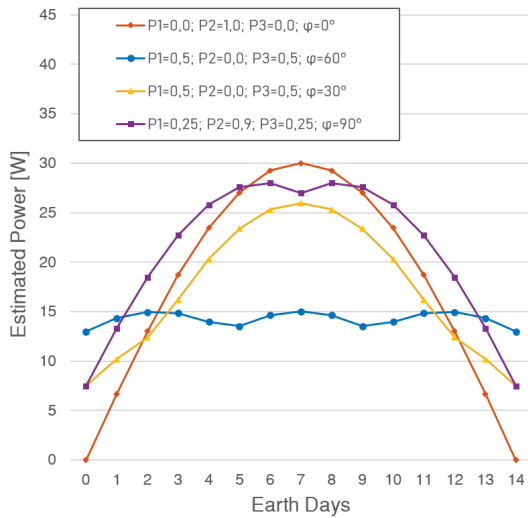
Fig. 11: Estimated power generation for different rover configurations. The reference panel has a power of 30W under moonlight conditions. Total energy values: *red:* 6.4 kWh *blue:* 5.1 kwH, *yellow:* 6.2 kWh, *purple:* 7.5 kWh. *Legend:* The Value after P is the percentage of the reference panel used, May not sum up to 100 % due to different potential panel area, φ describes the side panels angel to the ground surface

5.3 Battery

According to Section 4, a capacity of approx. 1600 Wh will be necessary to survive the lunar night. The cell types chosen are terrestrial high density LiPo cells which provide 192 Wh/kg in an 8C configuration. Considering margins for mounting and cables, this results in a total battery mass of 9 kg.

6. Locomotionn and Structure

6.1 Locomotion

While the initial idea was to build a four-wheeled rover as currently proposed by many state-of-the-art system designs, based on friction estimation analysis [19] [20] it was decided to use a six-wheeled locomotion system, as used in the Pathfinder and Chandrayaan-3 rovers. Table 3 shows a comparison of different concepts from the literature. The mass has been estimated based on the required elements such as actuators, wheel size, rods and differentials and then normalised for comparison. It can be seen that six-wheeled systems can achieve similar masses to a four-wheeled system. However, the actuators and wheels could be half the size, compensating for the higher number of elements required for a six-wheel
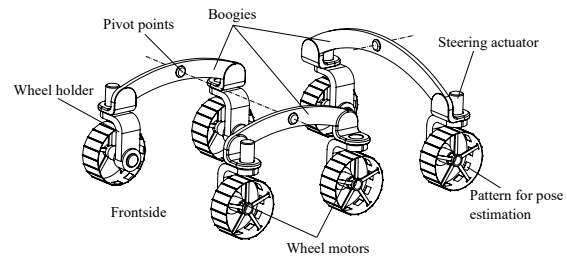

Fig. 12: Configuration for the SAMLER-KI rover locomotion system

Table 3: Locomotion concept comparison for climbing an object with 1 wheel

Concept	Friction needed	Estimated mass
4-Wheeler [19]	1,4	100%
MER [20]	0,65	103%
CRAB [20]	0,68	111%
RCL-E [20]	0,87	138%
3-Boogies [21]	0,65	102%

system. In addition, smaller elements allow a reduction in packaging size due to better accommodation. Avoiding skid steering is also an advantage over a four-wheel system.

To reduce the differential gear in the rover body needed for the rocker bogie configuration, it was decided to use the simpler transverse bogie configuration (3 boogies) as proposed for the ESA Exo Mars rover [21] and also used for the DFKI ARTEMIS rover [22] in 2014.

Finally, the locomotion system will include 6 wheel motors, 4 steering motors and 3 boogies, as shown in Figure 12. The design of the locomotion system is planned to be foldable, which can be achieved by snap-in mechanisms inside the pivot mounts. A total mass of 1.5 kg is targeted for the actuators, and an additional 1.6 kg for the structural elements.

Actuators Since the actuators are not thermally controlled, they have to cope with harsh demands on temperature ranges (Section 4). Since hall effect sensors are not able to withstand the night temperatures, sensor-less commutation methods have to be selected. Back-EMF or High Frequency-Injection methods are proposed as commutation technology to be used. In the simplest case, the steering motors can be controlled in stepper mode.

The steering mechanism will use the same actuators as the wheel drives, since the output torque requirements are similar. The steering angle will be
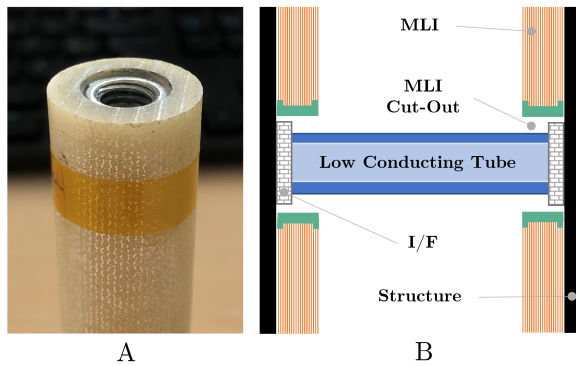
Fig. 13: *A:* Example of a GFRP Tube with threaded insert; *B:* Dual compartment spacer concept

Table 4: Estimated mass budget for the SAMLER-KI rover

Components		Mass [kg]
Mechanic	Loc. Structure	1.6
	Actuators	1.5
	Wheels	0.9
	Outer chassis	1.7
	Inner structure	0.9
Electronics	Main components	1.5
	Cameras	0.5
	Harness	0.5
	Battery	9
	Solar cells	0.25
TCS	MLI	2.1
	Radiator	0.35
	Thermal switch	0.4
Payload		0.5
Other	Antenna, Hinges, Releases, Mountings	1
Total		22.7

measured by a potentiometer and via the odemetry of the hazard detection cams. For this purpose, it is planned to integrate a mechanical pattern on the inside of the wheels, which can be detected by the cameras.

As mentioned in Section 3, terrestrial actuators are chosen for implementation in the functional demonstrator. A suitable candidate is a combination of a Maxon GPX 22-UP 4-stage ceramic gearbox with an ECX-Flat22-S motor, capable of achieving 4.5 Nm of torque and a desired maximum speed of $0.1 m/s$ on a flat surface, while having a mass of 130 g each. With a wheel diameter of 130 mm, the rover will have a theoretical maximum drive force of 70 N per wheel to perform GNC and locomotion tests under Earth gravity. An alternative design could be a custom development based on a Harmonic Drive HFUC-2A-8 gearbox with a Robodrive ILM-25 motor, originally designey for the DFKI RH5-Manus robot's gripping system. Weighing 137,5 g and equipped with space suitable components it would be an alternative after changing lubrication and output bearings.

6.2 Structure

The current concept approach is to use aluminium structures that are easy to manufacture and also achieve good lightweighting values. To refine the design, semi-finished products such as honeycombs and topology optimised parts will be used to reduce mass. As mentioned in Section 4, there will be an outer structure and an inner structure providing thermal insulation between the surface exposed to the environment and the thermally controlled inner structure. The conductive insulation shall be structurally achieved by the use of multiple low conduc-

tivity tubes, such as GFRP, connecting both compartments as shown in Figure 13. The junctions for the low conductivity tubes shall be designed to allow thermo-mechanical deformation to compensate for temperature differences of at least 140 K.

Table 4 gives an overview of the estimated mass budget. With the current design considerations, a mass of about 23 kg is estimated for the rover system. Further mass reduction is planned in future design iterations to meet the key requirement of less than 20 kg total mass (see Table 1).

7. **Onboard Data Handling (OBDH)**

The proposed computer and network architecture of the micro rover is depicted in Figure 14. There are two computers foreseen to control the entire system. One on-board computer (OBC), based on a SAMV71 microcontroller unit (MCU), acts as a system supervisor, controlling all the subsystems. A second GNC computer based on a system-on-chip (SoC) to implement specific guidance, navigation and control tasks. Communication with higher data rate systems such as payload, cameras and high speed communication link is established via Ethernet. Low level communication with actuators, sensors, mechanisms, etc. is established via a field bus or directly connected to the OBC. It implements low level system control and communication with actuators, sensors, mechanisms, etc. via a field bus or directly connected. The OBC
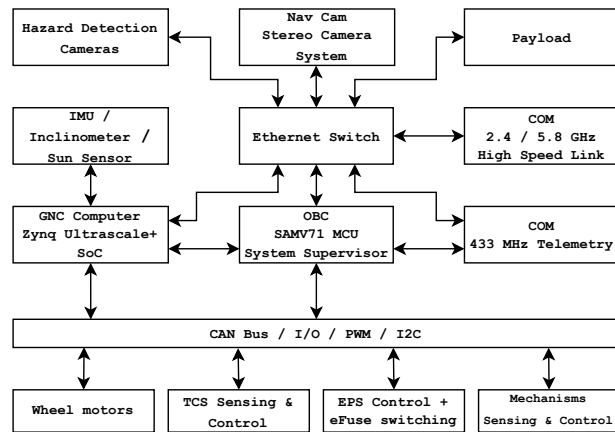
Fig. 14: Overview of the computer network architecture

Fig. 15: Overview of the System architecture

can be considered as always on, therefore depending on the mission state an extreme low power mode is foreseen.

7.1 Communication

Although the system is designed to be highly autonomous, communication with the ground station is necessary. Two separate communication links are provided for this purpose. A low level communication link for TM/TC and a second high speed data link for payload data such as high resolution camera data.

7.2 Software

The rover's software architecture depicted in Figure 15 is built around multiple subsystems that operate independently of each other at the control level. They can therefore be switched on or off depending on the current mission objectives for optimal power management. This design results in a higher level of resilience; even if some subsystems fail, the rover could still autonomously archive objectives with the remaining subsystems.

8. Guidance Navigation and Control (GNC)

The GNC requires localization and mapping of the environment implemented on the GNC computer using multiple sensor inputs for perception and state estimation. An important design driver for the selection of sensors and compute nodes as well as for the design of the software architecture was the limited mass and power budget. When selecting electronic components, hardware functionally equivalent to spaceflight components shall be used.
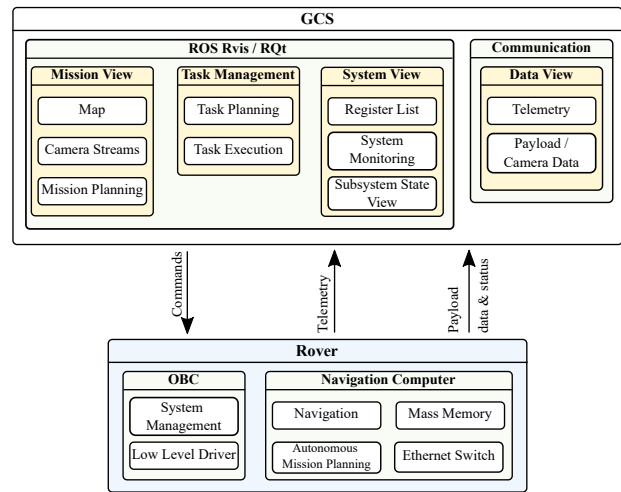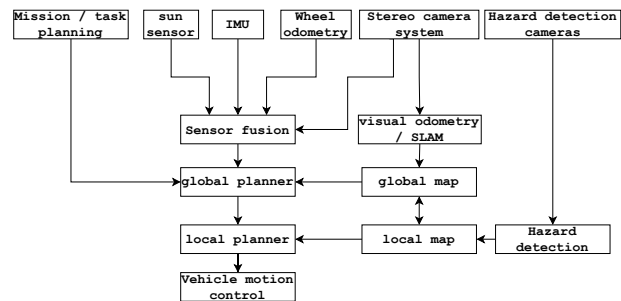

Fig. 16: Overview of the Navigation Hardware and Software stack

8.1 Hardware

The navigation hardware and software stack is depicted in Figure 16.

The selected GNC computer is based on a Xilinx Zynq Ultrascale+ SoC equipped with a stereo camera system and two separate hazard detection cameras in forward and backward direction. Furthermore, an inertial measurement unit (IMU), inclinometer, and sun sensor are envisaged.

8.2 Navigation software

The navigation software is based on the ROS 2 navigation stack and build with visual odometry at its core. The software architecture has a high similarity with the architecture of the MMX rover by DLR [23]. It also focuses on visual odometry (VO) and simultaneous localization and mapping (SLAM) using a stereo camera system and multiple cameras to check the wheels as its planed for the SAMLER-KI rover.

Table 5: A subset of evaluated SLAM algorithms

Algorithm	Sensor	Method
DXSLAM	mono, stereo, RGBD	feature-based CNN-SLAM
YPD-SLAM	RGB	ORB, CAPE-planes, Yolo-FastestV2
OrbSLAM3	mono, stereo, RGBD	ORB-features, descriptors

SAMLER-KI's rover positioning and navigation system uses only cameras because of their versatility, light weight and the fact that they don't have any moving parts that could be damaged or destroyed during take-off or flight. Two hazard detection cameras at the front and rear of the rover are used to inspect the wheels, perform vison-based odometry and obstacle detection, while the main stereo camera system in the upper front provides imagery for autonomous localisation and navigation. Vision-based algorithms will be used for visual odometry and visual SLAM for navigation and localisation. Here, Orb-SLAM3 has been pre-selected as the most promising algorithm for visual navigation.

As the basis for the navigation system, the Robot Operating System (ROS) 2 nav2 navigation stack will be used for implementing the navigation on the rover. Thus, the navigation will benefit by its ability to generate global and local cost maps.

To benchmark, what algorithm would work best for GNC within the lunar environment, we evaluated multiple SLAM and VO algorithms 5. Criteria are: Power consumption, stability, hardware integration, performance, resource utilization and performance under different light conditions. One challenge identified within the survey is, that many studies using data from indoor offices or roads of the big data sets behind, which are not comparable to a sparse environment in terms of features on the lunar surface. For our scenario, the following algorithms were found to be the most appropriate.

DXSLAM [24] has been published in 2020 and is using a Convolutional Neural Network to detect features and achieves greater accuracy then OrbSLAM 2.

YPD-SLAM [25] is a new algorithm that has been published in 2022. It utilizes deep neural network-based techniques to get a high accuracy to detect features. It is trained on indoor environments and might get good results for a static lunar environment.

OrbSLAM3 [26] is the first real-time SLAM which is able to perform visual, visual-inertial as well as multi-map SLAM. It is able to run on monocular, stereo and RGB-D cameras. The library is characterized in all sensor configurations by its robustness and accuracy under different lightning conditions and environments also on resource constrained systems.

The most important factors we have identified for the further development and implementation of the GNC stack is the sparse environment on the lunar surface with sometimes difficult exposure conditions and worse feature detection compared to urban environments. Furthermore, the limited resources of the GNC computer pose a challenge. On the one hand the limited RAM, limiting the size of the map, and on the other hand the computing power.

The challenge with the map size could be solved for example with a rolling map. This means that the map is only held in memory for a limited radius around the rover. For points outside this radius only the way points of the travelled trajectory would be stored to be able to return to the origin, e.g. to the lander.

The computational power of the selected GNC computer should be utilized as best by accelerating parts of the SLAM algorithm in hardware. For this purpose, parallelizable parts are particularly suitable to be implemented in the FPGA. This requires a detailed investigation and profiling of the implementation to identify computational intensive sections. Furthermore, the independence of data of these code sections is required to apply techniques like loop or pipelining.

To improve the feature detection in sparse environments, we plan to utilize a hybrid approach to use the visual SLAM in combination with neuronal networks trained for robust feature detection in sparse environments. This approach is heavily dependent on relevant data sets and is especially a challenge in the space sector as the community is lacking of open data sets. Therefore, we have setup a photo-realistic simulation environment for simulation and generation of imagery data. This can not seen as a replacement for real imagery data but is a good trade-off for the first iterations.

9. Verification

9.1 Models

As the SAMLER-KI project is still in its early stages, the functional demonstrator design will be completed by the end of 2023. It will be used for analysis and correlation with the final demonstrator model used for testing GNC in 2025. Further, it is
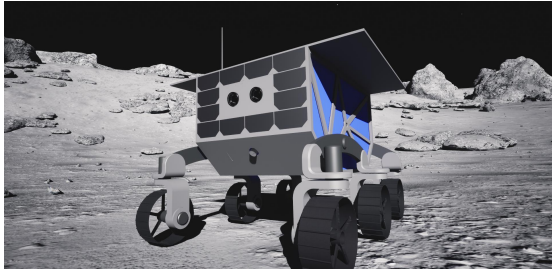
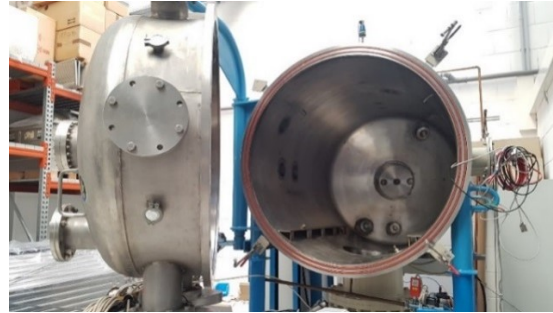Fig. 17: SAMLER-KI rover in lunar environment simulation

Fig. 18: VK2200 at FH Aachen

Fig. 19: Spacehall at DFKI

planned to build a Structural-Thermal Model (STM) of the rover body to test the TCS concept in the thermal vacuum chamber (TVAC) chamber at FH Aachen. This model could also be used for structural testing on a shaker.

9.2 Analysis

Thermal simulation environment The thermal behaviour of the rover system and its TCS is analysed in the thermal simulation software ESATAN-TMS. As there is a significant radiative interaction between the rover and its environment, the lunar environment is thermally simulated. The thermal simulation environment is capable of representing the transient behaviour of the lunar surface and its thermal interaction with an arbitrary object placed on it, which can be imported. In addition, a trajectory can be defined for this object, allowing thermal simulation of the entire rover mission using the actual rover geometry. The simulation environment is based on actual lunar topography data from the Lunar Reconnaissance Orbiter for the area specified by the traverse path.

GNC simulation To test and benchmark the vision-based localisation and navigation algorithms, a simulation environment capable of generating photorealistic images in real time was developed. Epic Games, Inc.'s Unreal Engine, with its new Nanite feature, was used to create a configurable, realistic-looking lunar landscape based on images and videos from the Apollo missions. Because it is a virtual environment, it can give us the exact position of the camera, providing a ground truth that can be compared with the position calculated by the visual SLAM algorithm. The environment with a 3D model of the current rover design is shown in Figure 17.

9.3 Test facilities

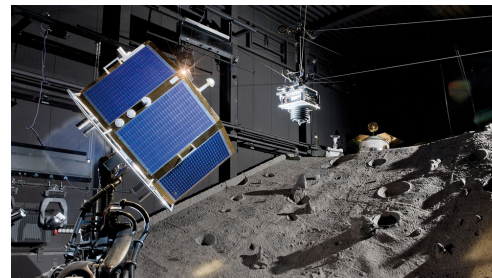**TVAC Chamber** The Thermal Vacuum Chamber VK2200 at FH Aachen, depicted in Figure 18, was designed to simulate the harsh environment of space conditions. Its internal envelope measuring approx. 900 mm in diameter and 1500 mm in length, providingthe capability to reach temperatures as low as -190°C and as high as +20°C. With a vacuum limit of less than 1×10^{-5} mbar, the chamber can accurately replicate the near-vacuum conditions on the lunar surface. For the most accurate representation of the lunar environment, the chamber utilises solar simulation capabilities, providing up to 1370W/m^2 of solar radiation, to allow testing of high temperature conditions. Dynamic thermal behaviour is provided by a variety of ground support equipment that enables the specimen to be actively rotated during the test, simulating different angles of solar incidence.

DFKI Space Exploration Hall The GNC tests will be conducted in DFKI's space exploration hall, providing an area of 105 m^2 of crater landscape. Six spotlights with active pan-tilt units for directional control provide realistic lunar light conditions with 14500 lux at 10 m in a color temperature of 6,000 K. Due to the possibility of influencing the shape of the light cones, precisely delimited areas of light and shadow can be created without any overlapping areas of light. The landscape provides slopes from 15° to 45° for experiments and a basing filled with sand for driving experiments in plane. With a ground truth

position measurement system integrated into the exploration hall, the rover's position and the performance of the SLAM algorithms can be monitored.

10. Conclusion and Outlook

Surviving the lunar night in a small system is no small feat. In the work described, a system design was conceptually developed to achieve this goal, taking a holistic view and considering detailed aspects for optimising individual subsystems. A concept for the thermal insulation of the rover system and storage of energy was developed and analysed, as well as a software and hardware architecture. Based on state-of-the-art SLAM algorithms, a GNC system has been designed, which is additionally capable of semi-autonomous control of the rover. Specialised simulation environments and test facilities for subsystem development and future verification of the results are also part of the work described.

Successful implementation and testing of the technologies described would provide lunar rovers the potential to multiply their range while greatly extending mission duration, travel distance and possible objectives.

Acknowledgment

References

[1] C. J. Cremers, R. C. Birkebak, and J. E. White, "Lunar surface temperatures from Apollo 12," *The Moon*, vol. 3, no. 3, pp. 346–351, 1971. DOI: 10.1007/bf00561846.

[2] European Space Agency, "ESA strategy for science at the moon," ESA, Tech. Rep., May 2019. [Online]. Available: http://exploration.esa.int/science-e/www/object/doc.cfm?fobjectid=61372.

[3] B. Betts, *Microrovers: Current and past examples and conclusions*, Microrover Space Horizons Workshop, Accessed 08.2023, Feb. 2012.

[4] C. G. Marirrodriga, M. Van Winnendael, and P. Putz, "Micro-rovers for scientific applications in mars or moon missions," Automation and Ground Facilities Division, ESTEC, 1997.

[5] *Microrovers for assisting humans*, Accessed 08.2023. [Online]. Available: https://www.planetary.org/sci-tech/microrovers-for-assisting-humans.

[6] A. Gemer, J. Cyrus, F. Meyen, and J. Cyrus, "Advances in lunar science return via distributed instrument mobility and swarm robotics: The lunar outpost mobile autonomous prospecting platform (MAPP) rovers," *LPI Contributions*, vol. 2635, p. 5018, 2021.

[7] J. Walker, "Flight system architecture of the sorato lunar rover," in *Proceedings of the International Symposium on Artificial Intelligence, Robotics and Automation in Space (i-SAIRAS 2018)*, Madrid, Spain, 2018, pp. 4–6.

[8] *Cuberover payload users guide v1.7*, Astrobotic Technology, 2021. [Online]. Available: https://www.astrobotic.com/wp-content/uploads/2021/07/CubeRover-Payload-Users-Guide-v1.7.pdf.

[9] B. Hülsen, P. Schöberl, and N. A. Mulsow, "Modular eps for small mobile robotic space systems," in *Accepted for Proceedings of the 13th European Space Power Conference – ESPC 2023*, Alicante, Spain, Oct. 2023.

[10] N. Mulsow, B. Hülsen, and P. Schöberl, "Towards influences of the eps on lunar rover's systems design," Jun. 2022.

[11] J. W. Krahwinkel, "Thermal-analyse zur konzepterstellung und evaluation eines mondrovers," M.S. thesis, Hochschule Bremen, Bremen, 2021.

[12] B. Hülsen, A. Dabrowski, N. A. Mulsow, W. Brinkmann, J. Guetzlaff, L. Spies, M. Czupalla, and F. Kirchner, "Towards an autonomous micro rover with night survivability for lunar exploration," in *Accepted for Proceedings of the 74th International Astronautical Congress (IAC)*, Baku, Azerbaijan, Oct. 2023.

[13] D. G. Gilmore, *Spacecraft Thermal Control Handbook*. The Aerospace Corporation, 2002, vol. 1.

[14] R. Peyrou-Lauga and P. Gautier, "JUICE (jupiter icy moon explorer) spacecraft thermal contro," in *50th International Conference on Environmental Systems*, ICES, 6.2021, pp. 11–12.

[15] *HPS-radiators*, Accessed 08.2023, May 2020. [Online]. Available: `https://www.hps-gmbh.com / portfolio / subsystem - integrals / radiators-2/`.

[16] *HiPeR; high performance radiator technology - flexible film radiator technology for spacecraft thermal management*, Airbus, May 2017.

[17] K. S. Novak, "Development of a thermal control architecture for the mars exploration rovers," *AIP Conference Proceedings*, 2003. DOI: `10.1063/1.1541295`.

[18] K. Shinozaki, T. Nohara, M. Ando, A. Okamoto, M. Maeda, H. Sugita, and S. Takada, "Research and development of heat switch for future space missions," *Transactions of the japan society for aeronautical and space sciences, Aerospace Technology Japan*, vol. 12, no. ists29, 2014. DOI: `10.2322/tastj.12.po_4_7`.

[19] D. Bickler, *The mars rover mobility system*, version V1, 1997. DOI: `2014/18908`. [Online]. Available: `https://hdl.handle.net/2014/18908`.

[20] T. Thueer, A. Krebs, and R. Siegwart, "Comprehensive locomotion performance evaluation of all-terrain robots," in *2006 IEEE/RSJ International Conference on Intelligent Robots and Systems*, 2006, pp. 4260–4265. DOI: `10.1109/IROS.2006.281954`.

[21] S. Michaud, A. Gibbesch, T. Thueer, A. Krebs, C. Lee, B. Despont, B. Schäfer, and R. Slade, "Development of the exomars chassis and locomotion subsystem," in *Proceedings of i-SAIRAS 2008 - 9th International Symposium on Artificial Intelligence, Robotics and Automation in Space*, Feb. 2008. [Online]. Available: `https://elib.dlr.de/55365/`.

[22] M. Manz, R. Sonsalla, J. Hilljegerdes, C. Oekermann, J. Schwendner, S. Bartsch, and S. Ptacek, "Mechanical design of a rover for mobile manipulation in uneven terrain in the context of the spacebot cup," in *International Symposium on Artificial Intelligence, Robotics and Automation in Space (iSAIRAS) Montreal*, Jun. 2014. DOI: `10.13140/2.1.1471.3920`.

[23] M. Vayugundla, T. Bodenmüller, M. J. Schuster, M. G. Müller, L. Meyer, P. Kenny, F. Schuler, M. Bihler, W. Stürzl, B.-M. Steinmetz, *et al.*, "The mmx rover on phobos: The preliminary design of the dlr autonomous navigation experiment," in *2021 IEEE Aerospace Conference (50100)*, IEEE, 2021, pp. 1–18.

[24] D. Li, X. Shi, Q. Long, S. Liu, W. Yang, F. Wang, Q. Wei, and F. Qiao, "DXSLAM: A robust and efficient visual slam system with deep features," in *2020 IEEE/RSJ International Conference on Intelligent Robots and Systems (IROS)*, 2020, pp. 4958–4965. DOI: `10.1109/IROS45743.2020.9340907`.

[25] Y. Wang, H. Bu, X. Zhang, and J. Cheng, "YPD-SLAM: A real-time vslam system for handling dynamic indoor environments," *Sensors*, vol. 22, no. 21, p. 8561, 2022.

[26] C. Campos, R. Elvira, J. J. G. Rodríguez, J. M. M. Montiel, and J. D. Tardós, "ORB-SLAM3: An accurate open-source library for visual, visual–inertial, and multimap slam," *IEEE Transactions on Robotics*, vol. 37, no. 6, pp. 1874–1890, 2021. DOI: `10.1109/TRO.2021.3075644`.